

Stellar Occultations with the 3.6-m DOT: Probing Planetary Atmospheres

Anandmayee TEJ^{1,*}, Bruno SICARDY², Nagarhalli Madhav ASHOK³ and Saurabh SHARMA⁴

¹ Indian Institute of Space Science and Technology, Thiruvananthapuram, 695547, Kerala, India

² LESIA, Observatoire de Paris, Université PSL, CNRS, Sorbonne Université, Université de Paris, 5 place Jules Janssen, 92195 Meudon, France

³ Physical Research Laboratory, Ahmedabad, 380009, Gujarat, India

⁴ Aryabhata Research Institute of Observational Sciences, Manora Peak, Nainital 263002, India

* Corresponding author: tej@iist.ac.in

This work is distributed under the Creative Commons CC-BY 4.0 Licence.

Paper presented at the 3rd BINA Workshop on “Scientific Potential of the Indo-Belgian Cooperation”, held at the Graphic Era Hill University, Bhimtal (India), 22nd–24th March 2023.

Abstract

The present paper (which is based on Sicardy et al. (2021)) discusses investigation of solar system bodies made possible by the simple yet powerful technique of stellar occultation. We focus on the stellar occultation by Pluto on 2020, June 6. The event was observed at Devasthal, Nainital, India in the I and H bands with the 1.3-m and 3.6-m telescopes, respectively. From the observed light curve, the surface pressure of Pluto’s atmosphere was constrained to $p_{\text{surf}} = 12.23^{+0.65}_{-0.38} \mu\text{bar}$. This indicates a continuing plateau phase since mid-2015 which is in excellent agreement with the prediction of Pluto volatile transport model of Meza et al. (2019). This result stresses the importance of coordinated stellar occultation observations with facilities like Devasthal Optical Telescope (DOT) and Himalayan Chandra Telescope (HCT) where a few minutes of observing time lead to high-impact science.

1. Introduction

Stellar occultations have proven to be a very powerful technique to study solar system objects with very high science to observing time ratio. A plethora of discoveries like detecting tenuous atmospheres and ring systems are well documented in literature. During these events, where a solar system body passes in front of a star, we essentially scan the body. Here, the spatial resolution is defined by the time resolution and depends on the relative speed of the body with respect to the star in the plane of the sky. This results in very high spatial resolutions (of the order of fraction of km) far exceeding the limits from classical imaging, thus allowing for precise estimation of sizes and shapes of solar system bodies. Further, Earth-based occultations are now established as a highly efficient method to probe atmospheres in the solar system.

Stellar flux variation when occulted by an object with an atmosphere is gradual due to differential refraction of the incoming stellar rays by the refractivity gradient of the atmosphere.

This bending of starlight has resemblance with gravitational lensing where the atmosphere here acts as a lens. Spherical atmospheres produce two stellar images at any moment, a primary image (or near-limb image) and a secondary (or far-limb) image. Multiple images are produced by non-spherical atmospheres. Differential refraction compresses the images perpendicular to the limb, while they are stretched parallel to the limb because of focusing caused by the limb curvature. The stretching increases as the chords approach the planet centre resulting in the central flash (the two images merge into one and form the gravitational lens equivalent of a luminous ‘Einstein–Chwolson ring’ around the body) when the stellar limb intersects the planet center. The observed light curves enable us to probe the atmosphere. An elaborate discussion on the principles and equations that govern stellar ray propagation in planetary atmospheres can be found in Sicardy (2023).

To complete the discussion on stellar occultations, if the Moon occults a distant star, the Fresnel diffraction pattern observed enables estimation of stellar sizes, detection of circum-stellar envelopes, discovery of binary systems, etc., at very high resolutions of 1–2 milliarcsec much beyond the theoretical diffraction limit of telescopes. In this paper, we focus on stellar occultation by Pluto.

1.1. Pluto’s atmosphere

The discovery of CH₄ frost on the surface of Pluto (Cruikshank et al., 1976) was a breakthrough observation that strongly suggested the presence of an atmosphere. The existence of a tenuous atmosphere was eventually established a decade later during stellar occultations observed in 1985 and 1988 (Brosch, 1995; Hubbard et al., 1988; Elliot et al., 1989). A major in-road in probing Pluto’s atmosphere was achieved with a series of occultation observations between 1988 and 2003 which unraveled a striking twofold expansion (Elliot et al., 2003; Sicardy et al., 2003). Subsequent to this, as Pluto moved in front of the Galactic centre, a cluster of occultation events occurred during 2002 and 2016, which greatly enhanced our knowledge regarding the structure, dynamics, and evolution of the atmosphere of Pluto.

Based on two occultations observed in July 2012 and May 2013, Dias-Oliveira et al. (2015) have conducted detailed modeling in the framework of a pure and clear (haze-free) N₂ atmosphere. The two high-SNR light curves analyzed in this paper, covering well-sampled occulting chords, constrained the density, temperature, and thermal gradient profiles between radii of ~ 1190 – 1450 km, corresponding to pressures between ~ 11 – 0.1 μ bar, respectively. Using a unique template thermal model, an increase of 6% in the pressure (significant at the 6σ level) was detected over the period of ~ 9.5 months separating the two occultations. This showed that Pluto’s atmosphere was still expanding, consistent with the analysis of Olkin et al. (2015). In a more recent paper, Meza et al. (2019) have consistently modeled eleven occultation light curves spanning almost three decades between 1988 and 2016. The data show a three-fold monotonic increase of Pluto’s atmospheric pressure over that period.

Pluto’s orbit has high eccentricity ($e = 0.26$) and obliquity (102° – 126°). As a consequence, Pluto receives significantly less (\sim three times) sunlight at aphelion as compared to perihelion, resulting in complex changes to its surface insolation and temperature. This severely affects

Table 1: Observation log.

	3.6-m (DOT)	1.3-m (DFOT)
Telescope Coordinates	79° 41' 3.6" E	79° 41' 6.1" E
(topocentric)	29° 21' 39.4" N	29° 21' 41.5" N
Altitude	2450 m	2450 m
Detector	TIRCAM2 Raytheon InSb array	ANDOR DZ436 camera
Filter ($\lambda/\Delta\lambda$, μm)	H (1.60/0.30)	I (0.85/0.15)
Exposure time/Cycle time (s)	5/5.336	1.7/2.507

the N₂ atmosphere, which is in vapor-pressure equilibrium with the surface N₂ ice. Sputnik Planitia, a large depression filled with N₂ ice, was discovered by the NASA New Horizons flyby in 2015. The sublimation of N₂ ice in the Sputnik Planitia is the main engine that controls the large annual pressure variation of Pluto's atmosphere as it orbits around the Sun. The observed increase of Pluto's atmospheric pressure can be explained by its recession from perihelion (reached in September 1989), while summer progressed over the Northern Hemisphere, exposing Sputnik Planitia to the solar radiation.

In this paper, we present the results derived from the occultation that occurred on 6 June 2020. This is a timely observation, as Meza et al. (2019) predict that the pressure should peak around that epoch, starting a decline that should last for two centuries under the combined effects of Pluto's recession from the Sun and the prevalence of the winter season over Sputnik Planitia. This is also an important benchmark as Pluto is moving away from the Galactic plane, making stellar occultations increasingly rare, and thus making this measurement decisive.

2. Observations and Data Analysis

2.1. Occultation observation

The campaign to observe the 6 June 2020 occultation event was organized under the framework of the Lucky Star project (<https://lesia.obspm.fr/lucky-star>) Details of the event is available in a dedicated Lucky Star project page (<https://lesia.obspm.fr/lucky-star/occ.php?p=31928>). The magnitudes of the occulted star (GAIA 6864932072159710592) in the I and H bands are ~ 12.3 and ~ 11.6 , respectively, while that of Pluto during the event were ~ 13.8 and ~ 13.3 , respectively. This makes the occulted star 1.5 mag brighter than the combined Pluto + Charon system, ensuring a significant drop of the total flux of star + Pluto + Charon.

Simultaneous observations were carried out using two telescopes of the Aryabhata Research Institute of Observational Sciences (ARIES) located at Devasthal. One telescope was the 1.3-m Devasthal Fast Optical Telescope (DFOT) operating in I band, and the other one was the 3.6-m ARIES Devasthal Optical Telescope (DOT) operating in H band. Several test runs were carried out on days prior to the event to measure the sampling time and minimize errors. The observation details are listed in Table 1. Observations were also planned with the 2-m Himalayan Chandra Telescope (HCT), Hanle, operated by the Indian Institute of Astrophysics, Bangalore, India. However, the event was clouded out at that site.

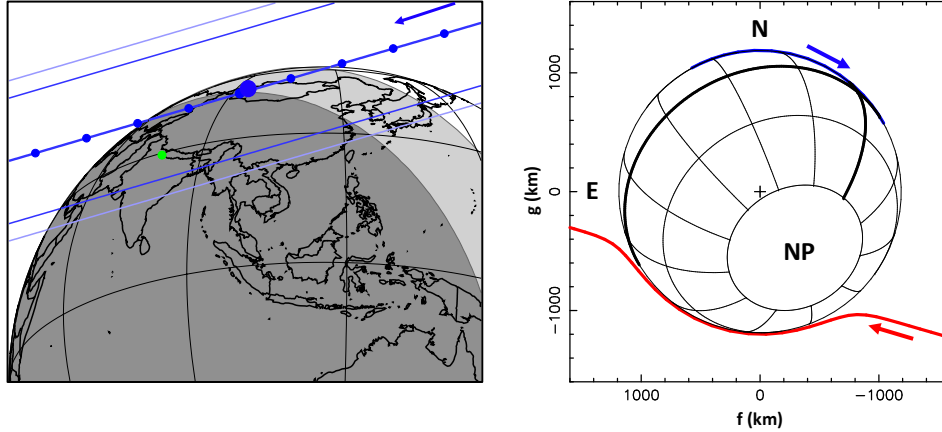


Figure 1: (left) The reconstructed, post-occultation path of Pluto’s shadow on 6 June 2020. The green dot is the location of Devasthal. The bullets on the shadow central line are plotted every minute, where the large one is for the geocentric closest approach time. The arrow indicates the direction of motion. The dark and light blue thinner lines are the shadow limits corresponding to the stellar half-light level and 1% stellar drop level (the practical detection limit), respectively. Dark gray regions of Earth are for astronomical night (Sun more than 18 deg below the horizon), while light gray regions are for astronomical twilight (Sun between 0 and 18 deg below the horizon). (right) Occultation geometry for the event, with the axes f and g being the offsets of the stellar images with respect to Pluto’s centre. The thick black lines are the equator and the prime (Charon-facing) meridian. The celestial north (N), celestial east (E) and Pluto’s North Pole are marked. Motion of the primary (red line) and secondary (blue line) stellar images relative to Pluto are shown. This figure is taken from Sicardy et al. (2021).

Figure 1 illustrates the derived reconstructed shadow path on Earth (left) and the corresponding geometry (right) of the occultation as seen from Devasthal. As discussed in Dias-Oliveira et al. (2015), the flux from two stellar images are actually recorded during the occultation. The flux from the primary stellar image dominates here, and it essentially scanned the northern, summer hemisphere of Pluto as seen from Devasthal. The observed light curves in the H and I bands observed with the 3.6-m and 1.3-m telescopes, respectively, are shown in Fig. 2.

3. Result and Discussion

3.1. Modelling Pluto’s atmosphere

To model Pluto’s atmosphere, we make the following assumptions: (i) it is spherically symmetric, (ii) is transparent (no haze), (iii) is an ideal gas in hydrostatic equilibrium, (iv) is composed of pure molecular nitrogen, N_2 , and (v) the temperature profile, $T(r)$, r being the distance from Pluto’s centre, is time-independent. The various parameters used in our fitting procedure are listed in Table 2. Considering the above assumptions, the observed light curves were fitted

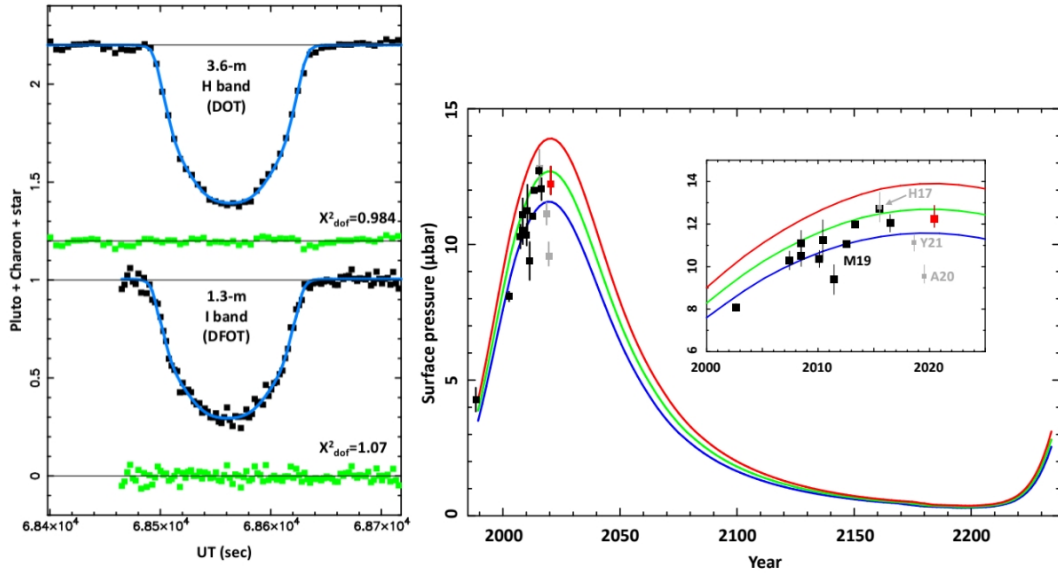


Figure 2: (left) The 6 June 2020 occultation light curve (black squares) and the best fit (blue curve) are shown for the Devasthal telescopes. The residuals (observation-minus-model) are plotted in green below each light curve. The lower and upper horizontal lines are the normalized total flux (star+Pluto+Charon) and the zero flux levels, respectively. The 3.6-m light curve has been shifted vertically by +1.2 for better viewing. (right) Evolution of Pluto’s atmospheric pressure between 1988 and 2020. Error bars are displayed at 1σ level. The black squares are the values published by Meza et al. (2019) (M19) and the red square is the result of the present work. The gray points in chronological order are: (1) H17, the New Horizons value from the radio science data occultation (ingress point, 14 July 2015, Hinson et al. (2017)) and coincides with the 29 June 2015 point from Meza et al. (2019); (2) Y21, the value derived by Young et al. (2021) from the ground-based, multi-chord 15 August 2018 occultation; and (3) A20, the result of Arimatsu et al. (2020) obtained from a grazing, single-chord occultation observed on 17 July 2019. The colored lines are the modeled annual evolution of the surface pressure obtained with the Pluto volatile transport model described in Meza et al. (2019). The blue, green and red curves correspond to N_2 ice albedos of 0.73, 0.725 and 0.72, respectively. The figure shown in both the left and right panels are taken from Sicardy et al. (2021).

Table 2: Adopted parameters for Pluto and its atmosphere.

Pluto's body	
GMass ¹	$GM_P = 8.696 \times 10^{11} \text{ m}^3 \text{ sec}^{-2}$
Radius ¹	$R_P = 1187 \text{ km}$
Geocentric distance	$4.97407 \times 10^9 \text{ km}$
Pluto's atmosphere	
N ₂ molecular mass	$\mu = 4.652 \times 10^{-26} \text{ kg}$
N ₂ molecular refractivity ²	$K = (1.091 \times 10^{-23} + 6.282 \times 10^{-26} / \lambda_{\mu\text{m}}^2) \text{ cm}^3 \text{ molecule}^{-1}$

¹ The values for GMass and Radius are taken from Stern et al. (2015), where G is the constant of gravitation.

² The value for refractivity is taken from Washburn (1930), where $\lambda_{\mu\text{m}}$ is the wavelength expressed in microns.

following the method described in Dias-Oliveira et al. (2015). This is an iterative process that combines both direct ray-tracing and Abel inversion. The inversion algorithm is first implemented to retrieve the atmospheric density, pressure, and temperature profiles of Pluto. Using these as input, synthetic light curves are generated through direct ray-tracing which are simultaneously fitted to the observed light curves. Subsequently, the inversion of the best fit light curve is done, and the iterative process continues which finally gives the density, pressure, and temperature profiles.

There are four adjusted parameters (M) in our model. These are p_{surf} , the pressure at Pluto's surface and $\Delta\rho$, the ephemeris offset perpendicular to Pluto's apparent motion projected in the sky. The other two parameters (ϕ_0 s) are the Pluto+Charon contribution to the two individual light curves. Since no calibration data was possible due to less than optimal sky conditions prevailing, these last two parameters are not known. Another parameter, the time shift Δt , that needs to be applied to Pluto's ephemeris for the best fit. Δt accounts for the ephemeris offset as well as the errors in the occulted star position and finally yields the time $t_{C/A,G}$ which gives the closest approach of Pluto to the star in the sky plane, as seen from the geocenter.

The best fit to the data are shown in Fig. 2 and the best fit parameters are listed in Table 3. The fitting was carried out simultaneously to the light curves obtained at the 3.6-m and 1.3-m telescopes over a 320-s interval covering the event. For a quantitative assessment of the quality of the fit, we use the function, $\chi^2 = \sum_1^N ((\phi_{i,\text{obs}} - \phi_{i,\text{syn}}) / \sigma_i)^2$. Here, σ_i is the noise level (measured by the standard deviation of the signal) of each of the N data points. $\phi_{i,\text{obs}}$ and $\phi_{i,\text{syn}}$ are the observed and synthetic fluxes at the i^{th} data point, respectively. Satisfactory fits are obtained for a χ^2 value per degree of freedom $\chi_{\text{dof}}^2 = \chi_{\text{min}}^2 / (N - M) \sim 1$, where χ_{min}^2 is the minimum value of χ^2 obtained in the fitting procedure. The model is sensitive to regions above 30 km altitude, so the retrieved pressure is for the radius 1215 km, $p_{1215} = 6.665_{-0.21}^{+0.35} \mu\text{bar}$. A factor of 1.837 is then applied to convert this into p_{surf} (Meza et al., 2019).

Table 3: Best fit parameters. The quoted error bars are at the 1σ level.

Fit results	
Surface pressure	$p_{\text{surf}} = 12.23_{-0.38}^{+0.65} \mu\text{bar}$
Geocentric closest approach distance to shadow center ¹	$\rho_{\text{C/A,G}} = +6044_{-7}^{+15} \text{km}$
Geocentric closest approach time to shadow center ²	$t_{\text{C/A,G}} = 19:01:02.40 \pm 0.14 \text{ s UT}$

¹ A positive value means that the shadow center went north of the Geocenter.

² Although the quoted error bar is small, a systematic error of the order of 1 s may be present in $t_{\text{C/A,G}}$ (see text).

4. Pressure Evolution in Pluto's atmosphere

The right panel of Fig. 2 illustrates the pressure evolution between 1988 and 2020. Increase in pressure is seen between 1988 and 2013, and it has reached a plateau regime since 2015. The 6 June 2020 occultation (red square) shows the prevailing stationary phase, which is in excellent agreement with the Pluto volatile transport model described in Meza et al. (2019) and does not reconcile with the sudden decrease in pressure reported by Young et al. (2021) and Arimatsu et al. (2020). A careful comparison of the methodology used by these authors need to be carried out to resolve the observed inconsistency.

5. Concluding Remarks

The results on Pluto's atmosphere presented in this paper clearly shows the potential of the technique of stellar occultation in probing atmospheres of minor bodies of the solar system with high spatial resolution and μ -bar level pressure sensitivity, which is not possible from classical imaging observations. The team has observed one such occultation event of Triton, the largest of Neptune's satellites, on 6 October 2022. The results based on this (Sicardy et al. in prep) will enable us to better understand the seasonal evolution of Triton's atmosphere. In particular, this study will confirm or discard the prediction by Bertrand et al. (2022) that Triton's surface pressure should slowly decrease in the forthcoming years.

Further Information

Authors' ORCID identifiers

0000-0001-5917-5751 (Anandmayee TEJ)

0000-0003-1995-0842 (Bruno SICARDY)

0009-0009-1831-3914 (Nagarhalli Madhav ASHOK)

0000-0001-5731-3057 (Saurabh SHARMA)

Author contributions

This work is part of a collective effort where all co-authors provide contributions.

Conflicts of interest

The authors declare no conflict of interest.

References

- Arimatsu, K., Hashimoto, G. L., Kagitani, M., Sakanoi, T., Kasaba, Y., Ohsawa, R. and Urakawa, S. (2020) Evidence for a rapid decrease of Pluto's atmospheric pressure revealed by a stellar occultation in 2019. *A&A*, 638, L5. <https://doi.org/10.1051/0004-6361/202037762>.
- Bertrand, T., Lellouch, E., Holler, B. J., Young, L. A., Schmitt, B., Marques Oliveira, J., Sicardy, B., Forget, F., Grundy, W. M., Merlin, F., Vangvichith, M., Millour, E., Schenk, P. M., Hansen, C. J., White, O. L., Moore, J. M., Stansberry, J. A., Oza, A. V., Dubois, D., Quirico, E. and Cruikshank, D. P. (2022) Volatile transport modeling on Triton with new observational constraints. *Icar*, 373, 114764. <https://doi.org/10.1016/j.icarus.2021.114764>.
- Brosch, N. (1995) The 1985 stellar occultation by Pluto. *MNRAS*, 276(2), 571–578. <https://doi.org/10.1093/mnras/276.2.571>.
- Cruikshank, D. P., Pilcher, C. B. and Morrison, D. (1976) Pluto: Evidence for Methane Frost. *Sci*, 194(4267), 835–837. <https://doi.org/10.1126/science.194.4267.835>.
- Dias-Oliveira, A., Sicardy, B., Lellouch, E., Vieira-Martins, R., Assafin, M., Camargo, J. I. B., Braga-Ribas, F., Gomes-Júnior, A. R., Benedetti-Rossi, G., Colas, F., Decock, A., Doressoundiram, A., Dumas, C., Emilio, M., Fabrega Polleri, J., Gil-Hutton, R., Gillon, M., Girard, J. H., Hau, G. K. T., Ivanov, V. D., Jehin, E., Lecacheux, J., Leiva, R., Lopez-Sisterna, C., Mancini, L., Manfroid, J., Maury, A., Meza, E., Morales, N., Nagy, L., Opitom, C., Ortiz, J. L., Pollock, J., Roques, F., Snodgrass, C., Soulier, J. F., Thirouin, A., Vanzi, L., Widemann, T., Reichart, D. E., LaCluyze, A. P., Haislip, J. B., Ivarsen, K. M., Dominik, M., Jørgensen, U. and Skottfelt, J. (2015) Pluto's Atmosphere from Stellar Occultations in 2012 and 2013. *ApJ*, 811(1), 53. <https://doi.org/10.1088/0004-637X/811/1/53>.
- Elliot, J. L., Ates, A., Babcock, B. A., Bosh, A. S., Buie, M. W., Clancy, K. B., Dunham, E. W., Eikenberry, S. S., Hall, D. T., Kern, S. D., Leggett, S. K., Levine, S. E., Moon, D. S., Olkin, C. B., Osip, D. J., Pasachoff, J. M., Penprase, B. E., Person, M. J., Qu, S., Rayner, J. T., Roberts, L. C., Salyk, C. V., Souza, S. P., Stone, R. C., Taylor, B. W., Tholen, D. J., Thomas-Osip, J. E., Ticehurst, D. R. and Wasserman, L. H. (2003) The recent expansion of Pluto's atmosphere. *Nature*, 424(6945), 165–168. <https://doi.org/10.1038/nature01762>.
- Elliot, J. L., Dunham, E. W., Bosh, A. S., Slivan, S. M., Young, L. A., Wasserman, L. H. and Millis, R. L. (1989) Pluto's atmosphere. *Icar*, 77(1), 148–170. [https://doi.org/10.1016/0019-1035\(89\)90014-6](https://doi.org/10.1016/0019-1035(89)90014-6).
- Hinson, D. P., Linscott, I. R., Young, L. A., Tyler, G. L., Stern, S. A., Beyer, R. A., Bird, M. K., Ennico, K., Gladstone, G. R., Olkin, C. B., Pätzold, M., Schenk, P. M., Strobel, D. F., Summers, M. E., Weaver, H. A. and Woods, W. W. (2017) Radio occultation measurements

of Pluto's neutral atmosphere with New Horizons. *Icar*, 290, 96–111. <https://doi.org/10.1016/j.icarus.2017.02.031>.

Hubbard, W. B., Hunten, D. M., Dieters, S. W., Hill, K. M. and Watson, R. D. (1988) Occultation evidence for an atmosphere on Pluto. *Natur*, 336(6198), 452–454. <https://doi.org/10.1038/336452a0>.

Meza, E., Sicardy, B., Assafin, M., Ortiz, J. L., Bertrand, T., Lellouch, E., Desmars, J., Forget, F., Bérard, D., Doressoundiram, A., Lecacheux, J., Oliveira, J. M., Roques, F., Widemann, T., Colas, F., Vachier, F., Renner, S., Leiva, R., Braga-Ribas, F., Benedetti-Rossi, G., Camargo, J. I. B., Dias-Oliveira, A., Morgado, B., Gomes-Júnior, A. R., Vieira-Martins, R., Behrend, R., Tirado, A. C., Duffard, R., Morales, N., Santos-Sanz, P., Jelínek, M., Cunniffe, R., Querel, R., Harnisch, M., Jansen, R., Pennell, A., Todd, S., Ivanov, V. D., Opatom, C., Gillon, M., Jehin, E., Manfroid, J., Pollock, J., Reichart, D. E., Haislip, J. B., Ivarsen, K. M., LaCluyze, A. P., Maury, A., Gil-Hutton, R., Dhillon, V., Littlefair, S., Marsh, T., Veillet, C., Bath, K. L., Beisker, W., Bode, H. J., Kretlow, M., Herald, D., Gault, D., Kerr, S., Pavlov, H., Faragó, O., Klös, O., Frappa, E., Lavayssière, M., Cole, A. A., Giles, A. B., Greenhill, J. G., Hill, K. M., Buie, M. W., Olkin, C. B., Young, E. F., Young, L. A., Wasserman, L. H., Devogèle, M., French, R. G., Bianco, F. B., Marchis, F., Brosch, N., Kaspi, S., Polishook, D., Manulis, I., Ait Moulay Larbi, M., Benkhaldoun, Z., Daassou, A., El Azhari, Y., Moulane, Y., Broughton, J., Milner, J., Dobosz, T., Bolt, G., Lade, B., Gilmore, A., Kilmartin, P., Allen, W. H., Graham, P. B., Loader, B., McKay, G., Talbot, J., Parker, S., Abe, L., Bendjoya, P., Rivet, J. P., Vernet, D., Di Fabrizio, L., Lorenzi, V., Magazzú, A., Molinari, E., Gazeas, K., Tzouganatos, L., Carbognani, A., Bonnoli, G., Marchini, A., Leto, G., Sanchez, R. Z., Mancini, L., Kattentidt, B., Dohrmann, M., Guhl, K., Rothe, W., Walzel, K., Wortmann, G., Eberle, A., Hampf, D., Ohlert, J., Krannich, G., Murawsky, G., Gährken, B., Gloistein, D., Alonso, S., Román, A., Communal, J. E., Jabet, F., deVisscher, S., Sérot, J., Janik, T., Moravec, Z., Machado, P., Selva, A., Perelló, C., Rovira, J., Conti, M., Papini, R., Salvaggio, F., Noschese, A., Tsamis, V., Tigani, K., Barroy, P., Irzyk, M., Neel, D., Godard, J. P., Lanoiselée, D., Sogorb, P., Vérilhac, D., Bretton, M., Signoret, F., Ciabattari, F., Naves, R., Boutet, M., De Queiroz, J., Lindner, P., Lindner, K., Enskonatus, P., Dangl, G., Tordai, T., Eichler, H., Hattenbach, J., Peterson, C., Molnar, L. A. and Howell, R. R. (2019) Lower atmosphere and pressure evolution on Pluto from ground-based stellar occultations, 1988-2016. *A&A*, 625, A42. <https://doi.org/10.1051/0004-6361/201834281>.

Olkin, C. B., Young, L. A., Borncamp, D., Pickles, A., Sicardy, B., Assafin, M., Bianco, F. B., Buie, M. W., de Oliveira, A. D., Gillon, M., French, R. G., Ramos Gomes, A., Jehin, E., Morales, N., Opatom, C., Ortiz, J. L., Maury, A., Norbury, M., Braga-Ribas, F., Smith, R., Wasserman, L. H., Young, E. F., Zacharias, M. and Zacharias, N. (2015) Evidence that Pluto's atmosphere does not collapse from occultations including the 2013 May 04 event. *Icar*, 246, 220–225. <https://doi.org/10.1016/j.icarus.2014.03.026>.

Sicardy, B. (2023) Study of atmospheres in the solar system, from stellar occultation or planetary transit. *CRPhy*, 23(S1), 213–241. <https://doi.org/10.5802/crphys.109>.

- Sicardy, B., Ashok, N. M., Tej, A., Pawar, G., Deshmukh, S., Deshpande, A., Sharma, S., Desmars, J., Assafin, M., Ortiz, J. L., Benedetti-Rossi, G., Braga-Ribas, F., Vieira-Martins, R., Santos-Sanz, P., Chand, K. and Bhatt, B. C. (2021) Pluto's Atmosphere in Plateau Phase Since 2015 from a Stellar Occultation at Devasthal. *ApJ*, 923(2), L31. <https://doi.org/10.3847/2041-8213/ac4249>.
- Sicardy, B., Widemann, T., Lellouch, E., Veillet, C., Cuillandre, J. C., Colas, F., Roques, F., Beisker, W., Kretlow, M., Lagrange, A. M., Gendron, E., Lacombe, F., Lecacheux, J., Birnbaum, C., Fienga, A., Leyrat, C., Maury, A., Raynaud, E., Renner, S., Schultheis, M., Brooks, K., Delsanti, A., Hainaut, O. R., Gilmozzi, R., Lidman, C., Spyromilio, J., Rapaport, M., Rosenzweig, P., Naranjo, O., Porras, L., Díaz, F., Calderón, H., Carrillo, S., Carvajal, A., Recalde, E., Caverro, L. G., Montalvo, C., Barría, D., Campos, R., Duffard, R. and Levato, H. (2003) Large changes in Pluto's atmosphere as revealed by recent stellar occultations. *Nature*, 424(6945), 168–170. <https://doi.org/10.1038/nature01766>.
- Stern, S. A., Bagenal, F., Ennico, K., Gladstone, G. R., Grundy, W. M., McKinnon, W. B., Moore, J. M., Olkin, C. B., Spencer, J. R., Weaver, H. A., Young, L. A., Andert, T., Andrews, J., Banks, M., Bauer, B., Bauman, J., Barnouin, O. S., Bedini, P., Beisser, K., Beyer, R. A., Bhaskaran, S., Binzel, R. P., Birath, E., Bird, M., Bogan, D. J., Bowman, A., Bray, V. J., Brozovic, M., Bryan, C., Buckley, M. R., Buie, M. W., Buratti, B. J., Bushman, S. S., Calloway, A., Carcich, B., Cheng, A. F., Conard, S., Conrad, C. A., Cook, J. C., Cruikshank, D. P., Custodio, O. S., Dalle Ore, C. M., Deboy, C., Dischner, Z. J. B., Dumont, P., Earle, A. M., Elliott, H. A., Ercol, J., Ernst, C. M., Finley, T., Flanigan, S. H., Fountain, G., Freeze, M. J., Greathouse, T., Green, J. L., Guo, Y., Hahn, M., Hamilton, D. P., Hamilton, S. A., Hanley, J., Harch, A., Hart, H. M., Hersman, C. B., Hill, A., Hill, M. E., Hinson, D. P., Holdridge, M. E., Horanyi, M., Howard, A. D., Howett, C. J. A., Jackman, C., Jacobson, R. A., Jennings, D. E., Kammer, J. A., Kang, H. K., Kaufmann, D. E., Kollmann, P., Krimigis, S. M., Kusnierkiewicz, D., Lauer, T. R., Lee, J. E., Lindstrom, K. L., Linscott, I. R., Lisse, C. M., Lunsford, A. W., Mallder, V. A., Martin, N., McComas, D. J., McNutt, R. L., Mehoke, D., Mehoke, T., Melin, E. D., Mutchler, M., Nelson, D., Nimmo, F., Nunez, J. I., Ocampo, A., Owen, W. M., Paetzold, M., Page, B., Parker, A. H., Parker, J. W., Pelletier, F., Peterson, J., Pinkine, N., Piquette, M., Porter, S. B., Protopapa, S., Redfern, J., Reitsema, H. J., Reuter, D. C., Roberts, J. H., Robbins, S. J., Rogers, G., Rose, D., Runyon, K., Retherford, K. D., Ryschkewitsch, M. G., Schenk, P., Schindhelm, E., Sepan, B., Showalter, M. R., Singer, K. N., Soluri, M., Stanbridge, D., Steffl, A. J., Strobel, D. F., Stryk, T., Summers, M. E., Szalay, J. R., Tapley, M., Taylor, A., Taylor, H., Throop, H. B., Tsang, C. C. C., Tyler, G. L., Umurhan, O. M., Verbiscer, A. J., Versteeg, M. H., Vincent, M., Webbert, R., Weidner, S., Weigle, G. E., White, O. L., Whittenburg, K., Williams, B. G., Williams, K., Williams, S., Woods, W. W., Zangari, A. M. and Zirnstein, E. (2015) The Pluto system: Initial results from its exploration by New Horizons. *Sci*, 350, aad1815. <https://doi.org/10.1126/science.aad1815>.
- Washburn, E. W. (1930) *International Critical Tables of Numerical Data, Physics, Chemistry and Technology*. The National Academies Press, Washington, DC. <https://doi.org/10.17226/>

20230.

Young, E., Young, L. A., Johnson, P. E. and PHOT Team (2021) More Evidence that Pluto's Atmosphere is Freezing Out: Central Flash Results from the 15-AUG-2018 Occultation. DPS, 53, 307.06.